

INVESTIGATION OF EEDF AND ELECTRON DENSITY AND TEMPERATURE BY DEVELOPED LANGMUIR PROBE IN RF-CCP ARGON DISCHARGE AND CORRELATION WITH OES

Djelloul MENDIL, Hadj LAHMAR, Laïd HENNI, Mounes ALIM, Djelloul LOUHIBI
and Karim HENDA

*Centre de Développement des Technologies Avancées, Cité du 20 août 1956, B.P. 17, Baba Hassen,
Alger, Algérie*

E-mail: dmendil@cdta.dz

ABSTRACT: The Langmuir probe, which was introduced for the first time by Langmuir and Mott-Smith [1], is a powerful mean for measuring the plasma parameters in low-pressure discharges. It allows a direct, local and absolute measurement of all plasma parameters (electron density and temperature, floating and plasma potential, and energy electron distribution function (EEDF)). A single rf-compensated cylindrical Langmuir probe has been developed in order to characterise a plasma RF discharge. Compensated measurements of EEDF and plasma parameters were conducted at powers ranging from 5 to 120 W and pressure of 0.3 mbar. The electronic density increases from 1.5×10^9 to $3.2 \times 10^{10} \text{ cm}^{-3}$ while the effective electron temperature decreases from 3.7 to 2.5 eV and then stabilizes beyond 70 W. They exhibit a transition between α and γ mode. The EEDFs were found to be Druyvesteyn-like below 70 W and then evolve to the Maxwellian beyond 70 W. OES method was applied to correlate with our Langmuir probe measurement. The intensities of the emission line at 7500 Å and 5145 Å follow the variation of n_e with power density, and then show a transition regime at the same power as the previous case.

KEYWORDS: cylindrical Langmuir probe, RF-CCP plasma discharge (13.56 MHz), RF compensation, EEDF, OES

1. Introduction

The Langmuir probe has been further investigated in various theoretical and experimental works [2,3]. In radiofrequency plasma where the parameters are modulated at the rf frequency, the conventional probe characteristic is no longer valid so the rf-compensation method must be used. In order to investigate the plasma parameters such as the electron density and temperature, the plasma and floating potential, and the EEDF, the single Langmuir probe is one of the most used techniques. In this paper we will investigate, by Langmuir probe, the experimental EEDF and the electron density and temperature at different RF power, and we will also investigate the intensity emission of argon atom and argon ion at different power, in order to find correlation between the two methods.

2. Experimental set-up

The schematic diagram of experimental setup used is shown in Figure 1. The apparatus consisted of a cylindrical vacuum vessel of stainless steel with 215 mm inner diameter and 204 mm height. The vacuum setting is ensured by a pumping installation. Inside the chamber two stainless steel circular plates (110 mm in diameter) serve as electrodes and the gap distance between them is fixed at 60 mm. One plate was grounded, while the other was subject to an applied RF voltage provided by an RF (13.56 MHz) power generator.

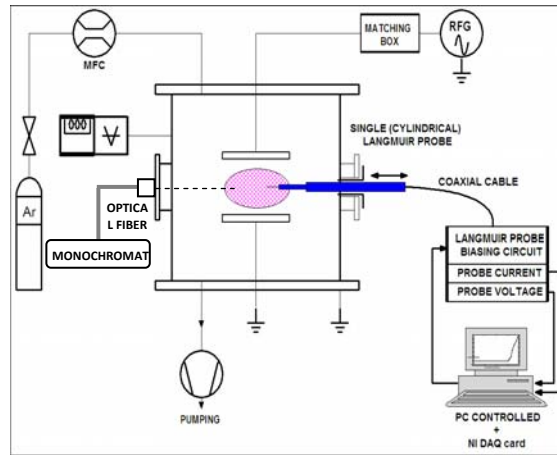


Figure 1 : Schematic diagram of experimental apparatus of CCP with the diagnosis by Langmuir probe and OES.

2.1. Langmuir probe construction

A movable (cylindrical) single Langmuir probe, shown in Figure 2, was built and introduced inside the chamber. The probe tip was 0.3 mm diameter tungsten wire exposing 7 mm long-tip to the plasma. A low thickness stainless steel cylinder is used as an rf-compensation electrode coupled via a 390 pF capacitor to the tungsten wire and to miniature self-resonant inductors which are assembled in series. The attenuation response of those chokes inductors at the fundamental, 2nd and 3rd harmonic is showed in figure 3. At the probe end was connected a data acquisition system added with a laboratory build measurement and power amplifier circuits.

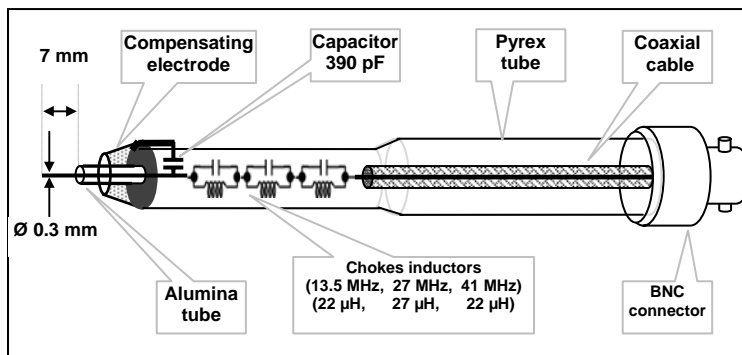


Figure 2 : Schematic diagram of cylindrical Langmuir probe.

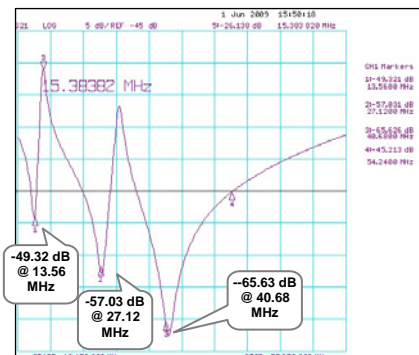


Figure 3 : The chokes inductors attenuation response at the fundamental, the 2nd and the 3rd harmonic.

2.2. Data acquisition

The data acquisition system consisted of NI PCI-6221 card and NI BNC-2120 terminal block added with a lab built measurement and power amplifier circuits. A LabVIEW VI was built to enable us to control all this system. This VI allowed us to choose the applied potential range, the voltage step, the measurement duration, the number of points, filters, and the sampling frequency. The current-voltage data were automatically backed up in text files for subsequent analysis. In our case, probe voltage was changed from -60 V to +60 V, and probe current was recorded (500 points) by measuring the voltage across a 100 ohm resistor at 1 s duration.

3. Probe analysis

The floating potential is the zero-crossing point of the experimental curve, Figure 4, $I=I_e+I_i=0$, where, I is the total probe current, I_e the electronic current, and I_i , the ionic current, Figure 5. The determination of the plasma potential is essential since it will be used as reference for all the following of the probe curve analysis. It is determined by the maximum of the first derivative (dI/dV) of the probe characteristic, or by the determination of the zero-crossing point of the second derivative (d^2I/dV^2) [4]. Before this operation, the data are smoothed to remove digital noise [5]. To obtain accurate values of electron density n_e and temperature T_e from the $I-V$ characteristic, the most difficulty is to separate the ion current I_i from the electron current I_e , in the region near the floating potential, where both contribute to the total current I . In our case, the orbital motion limit (OML) theory is found to be the well appropriate one since the squared ionic current was fitted linearly [6] as shown bellow in Figure 6. So, to subtract the I_i from I , Figure 5, we have used the OML ion current fit according to Equation 1 [1, 5]:

$$I_i = Aen_i \sqrt{\frac{kT_i}{2\pi m_i}} \frac{2}{\sqrt{\pi}} \sqrt{1 - \frac{eV}{kT_i}} \quad \rightarrow \quad I_i \xrightarrow{T_i \rightarrow 0} Aen_i \frac{\sqrt{2}}{\pi} \sqrt{\frac{eV}{m_i}} \quad (1)$$

where e , m_i , k , T_i , n_i , A , and V are respectively the elementary charge, ion mass, Boltzmann constant, ion temperature, ion density, probe area, and the probe voltage when taking the plasma potential as reference.

In the (I_e-V) semi-log plot, when $\ln(I_e)$ is not a straight line in the area located between the floating and the plasma potential, the EEDF, in this case, is not Maxwellian. The electron density n_e and the effective electron temperature T_{eff} [7] were determined from the Equation 2 and Equation 3 [4].

$$n_e = \int_0^{\varepsilon_{max}} G_e(\varepsilon) d\varepsilon \quad (2)$$

$$T_{eff} = \frac{2}{3n_e} \int_0^{\varepsilon_{max}} \varepsilon G_e(\varepsilon) d\varepsilon \quad (3)$$

$$G_e(V) = \frac{2m_e}{e^2 A} \sqrt{\frac{2eV}{m_e}} \frac{d^2 I_e}{dV^2} \quad (4)$$

Where $G_e(\varepsilon)$ and m_e are the energy distribution function and the electron mass, $\varepsilon=eV$.

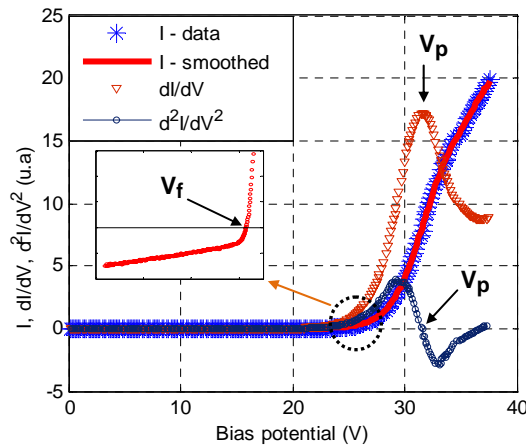


Figure 4 : $I-V$ probe curve (*), smoothed $I-V$ (---), first derivative dI/dV (▼) and second derivative d^2I/dV^2 (○)

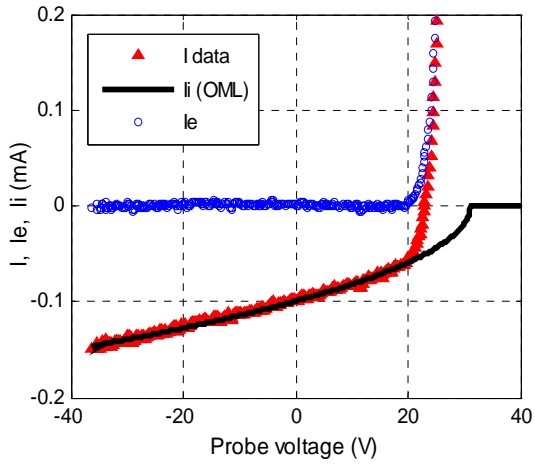


Figure 5 : OML extrapolation method of ionic current

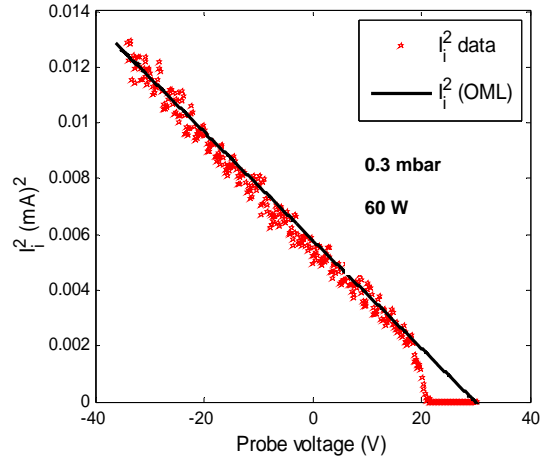


Figure 6 : Ionic current squared and its OML fit

4. Results and discussions

Since the EEDFs, which are determined from the equation 4, were used for determining the electron density and temperature, they have been studied. The explored EEDFs for all the cases of powers are shown in Figure 7 in linear scale, and their evolution shows a growth of their maximum amplitude as a function of increasing power. All these measurements were made at the center of the discharge at an argon pressure of 0.3 mbar.

The Figure 8 shows that the shape of these EEDFs in semi-log scale, are found to be predominantly Druyvesteyn-like below 70W, however, beyond this value the EEDFs evolving towards a Maxwellian. This reflects a transition of EEDFs from Druyvesteyn to a Maxwellian as showed in Figure 9 and Figure 10.

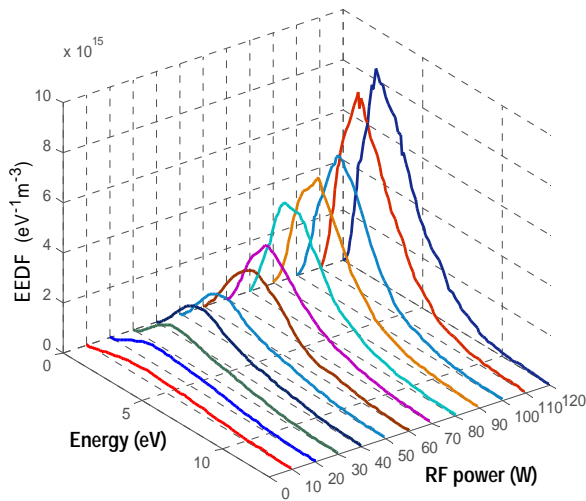


Figure 7 : experimental EEDFs for different rf powers at 0.3 mbar Ar pressure in linear scale

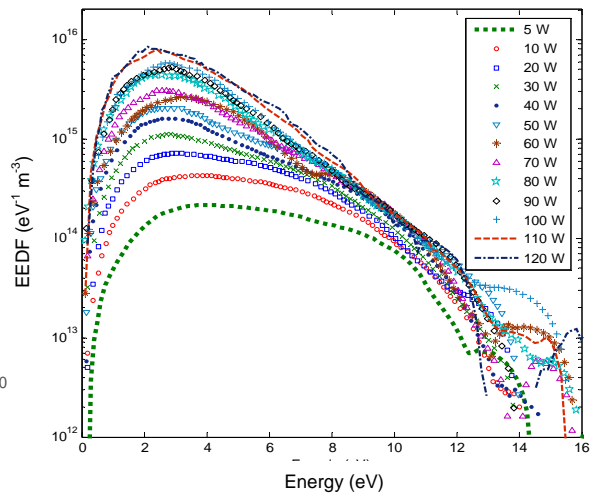


Figure 8 : experimental EEDFs for different powers at 0.3 mbar of argon pressure in semi-log scale

The Figure 9, shows an example of measured EEDF at a power of 30 W and a pressure of 0.3 mbar, compared with theoretical distributions plotted in the same experimental conditions, of electron density and effective temperature which are respectively 6.10^9 cm^{-3} and 2.7 eV. This figure shows clearly that the distribution is Druyvesteyn-like but not Maxwellian.

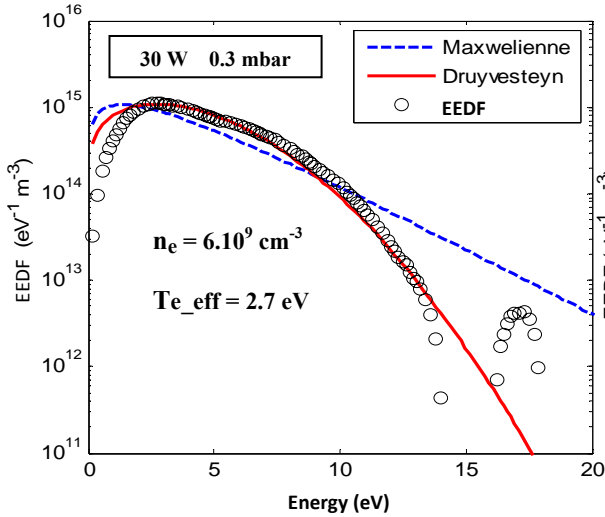


Figure 9 : experimental EEDF measured at 30 W power and 0.3 mbar argon pressure, with theoretical Druyvesteyn and Maxwell EEDF plotted in the same experimental conditions.

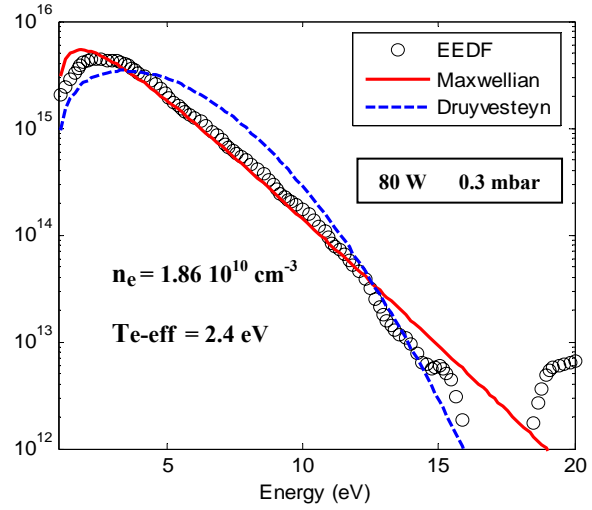


Figure 10 : Fit of experimental EEDF measured at 80 W and 0.3 mbar, by the Maxwellian one and the Druyvesteyn one.

The Figure 10 shows an example of the experimental FDEE, obtained for a power of 80 W, fitted by the theoretical EEDF of Druyvesteyn and Maxwell. Both theoretical EEDF are adjusted by varying the values of density and electron temperature until one of them close up or be superimposed on the experimental EEDF. This Figure shows that the EEDF closer to a Maxwellian than to a Druyvesteyn, but with an underestimation of the electron temperature of about 30%.

The evolution of density and effective electron temperature on a power range from 5 W to 120 W is shown in Figure 11. It shows a linear increase in density from $1.5 \times 10^9 \text{ cm}^{-3}$ to $3.2 \times 10^{10} \text{ cm}^{-3}$, while the effective temperature decreases from 3.75 eV to 2.35 eV. The latter undergoes a rapid decrease at low powers; however, at high powers it does not vary much. This behavior is a signature of a transition from α to γ regime in capacitively rf discharges. Similar results to ours are obtained by other authors [10,11].

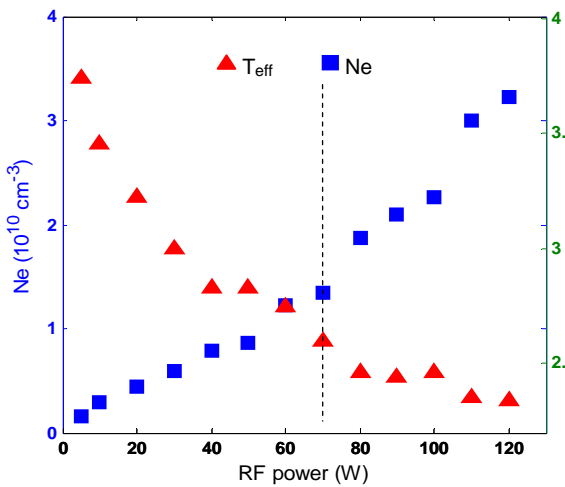


Figure 11 : Evolution of electron density and effective electron temperature at 0.3 mbar Ar pressure and at different rf powers.

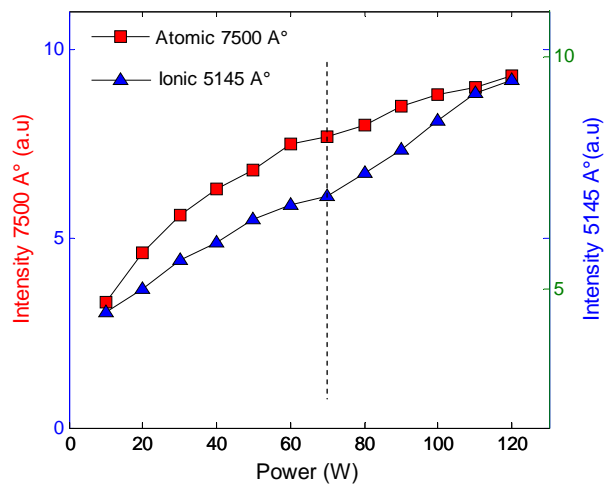


Figure 12 : Evolution of line intensities of argon atom (7500 Å°) and of argon ion (5145 Å°) versus power at 0.3 mbar argon pressure

We conducted a qualitative study of atomic emission intensity (7500 Å) and ionic emission intensity (5145 Å) of argon as a function of RF power and the results are shown in Figure 12. The purpose of this study is to find a qualitative correlation between the results of measurement by Langmuir probe and those obtained by emission spectroscopy. The intensity of an emission line depends on the transition probability, which is a physical quantity of the line, and on the population of the upper level. It is therefore possible to correlate the population density of an excited level, in our case Ar* or Ar⁺*, with the intensity of its corresponding ray. The emission intensity of atomic argon adopts faster growing at low powers than at high powers, and a change of pace of growth is more apparent at around 70 W. On the other hand, a slightly different behavior is observed for the intensity emission of argon ion. It feels almost linearly between 5W 70W and then the slope of growth increases slightly above 70 W as in the case of the evolution of the electron density previously discussed. We believe in trying to correlate with the results obtained by the Langmuir probe, this change in slope is due to the transition between the two regimes α and γ . It can be explained by the fact that in the γ regime, the emission of secondary electrons into plasma is increasingly important as the RF power increases and the energy of these electrons in the sheath increases as V_{de} increases, thereby increasing their efficiency of ionization and excitation. It increases the number of ions created by electron impact and the number of ion excited is depleting the number of neutral atom and excited atom.

5. Conclusion

The analysis of all of $I-V$ curves, measured in the range of 5–120 W, showed that the simple OML formula was found to fit the experimental data consequently the I_i^2-V plots are almost always exactly linears. To achieve this, a probe was designed and constructed with radius r_p as small as possible relative to Debye length and an appropriate data acquisition system and compensation method has been developed and operated. The formation of the EEDF was investigated experimentally in the center of the discharge, they were found to be Druyvesteyn-like in the range of 5–70 W and then evolve to the Maxwellian beyond 80 W. The behavior of electron density and temperature and of atomic and ionic emission intensity, exhibit a transition between the α heating mode operating at low powers, and the secondary-electron γ heating mode operating at high powers.

References

- [1] Mott-Smith H. M. and Langmuir I. ; *Phys. Rev.* **Vol. 28** pp 727-763 (1926)
- [2] Allen J. E., Boyd R. L. F. and Preynold P. ; *Proc. Phys. Soc. London*, 70B: 297 (1957)
- [3] Laframboise J. ; *Rept. 100* ; University of Toronto Institute for Aerospace studies (1966)
- [4] Lieberman M. A. and Lichtenberg A. J. ; Wiley ; New York (1994)
- [5] Chen F. F. ; *Physics of Plasmas* **Vol. 8** pp. 3029-3041 (2001)
- [6] Chen F. F. ; *Plasma Sources Sci. Technol.* **Vol. 18** p. 035012 (2009)
- [7] Godyak V. A. and Piejak R. B. ; *J. Appl. Phys.* **Vol. 73** pp. 3657-3663 (1993)
- [8] Dyson A., Bryant P. and Allen J. E. ; *Meas. Sci. Technol.* **Vol. 11** pp. 554-559 (2000)
- [9] Kortshagen U. and Schluter ; *J. Phys. D: Appl. Phys.* **Vol. 24** pp. 1585-1593 (1991)
- [10] Tatanova M., Thieme G. et al.; *Plasma Sources Sci. Technol.* **Vol. 15** pp. 507-516 (2006)
- [11] V. A. Godyak, R. B. Piejak, B. M. Alexandrovich, *Phys. Rev. Lett.* **Vol. 68** pp. 40-43 (1992)